

New avenue to the Parton Distribution Functions: Self-Organizing Maps

H. Honkanen^{a,b,*}, S. Liuti^{a,†}

^a*Department of Physics, University of Virginia, P.O. Box 400714,
Charlottesville, VA 22904-4714, USA*

^b*Department of Physics and Astronomy, Iowa State University,
Ames, IA 50011, USA*

J. Carnahan^c, Y. Loitiere^c, P. R. Reynolds^c

^c*Department of Computer Science, School of Engineering,
University of Virginia, P.O. Box 400740 Charlottesville, VA 22904-4740,
USA*

Abstract

Neural network algorithms have been recently applied to construct Parton Distribution Function (PDF) parametrizations which provide an alternative to standard global fitting procedures. We propose a technique based on an interactive neural network algorithm using Self-Organizing Maps (SOMs). SOMs are a class of clustering algorithms based on competitive learning among spatially-ordered neurons. Our SOMs are trained on selections of stochastically generated PDF samples. The selection criterion for every optimization iteration is based on the features of the clustered PDFs. Our main goal is to provide a fitting procedure that, at variance with the standard neural network approaches, allows for an increased control of the systematic bias by enabling user interaction in the various stages of the process.

PACS numbers: 13.60.Hb, 12.38.Bx, 84.35.+i

*heli@iastate.edu

†sl4y@virginia.edu

1 Introduction

Modelling experimental data always introduces bias, in the form of either a theoretical or systematical bias. The former is introduced by researchers with the precise structure of the model they use, which invariably constrains the form of the solutions. The latter form of bias is introduced by algorithms, such as optimization algorithms, which may favour some results in ways which are not justified by their objective functions, but rather depend on the internal operation of the algorithm.

In this paper we concentrate on high energy hadronic interactions, which are believed to be described by Quantum Chromodynamics (QCD). Because of the properties of factorization and asymptotic freedom of the theory, the cross sections for a wide number of hadronic reactions can be computed using perturbation theory, as convolutions of perturbatively calculable hard scattering coefficients, with non perturbative Parton Distribution Functions (PDFs) that parametrize the large distance hadronic structure. The extraction of the PDFs from experiment is inherently affected by a bias, which ultimately dictates the accuracy with which the theoretical predictions can be compared to the high precision measurements of experimental observables. In particular, the form of bias introduced by PDFs will necessarily impact the upcoming searches of physics beyond the Standard Model at the Large Hadron Collider (LHC). This situation has in fact motivated an impressive body of work, and continuous, ongoing efforts to both estimate and control PDFs uncertainties.

Currently, the established method to obtain the PDFs is the global analysis, a fitting procedure, where initial scale $Q_0 \sim 1\text{GeV} \leq Q_{\text{dat}}^{\text{min}}$ ansatz, as a function of the momentum fraction x , for each parton flavour i in hadron h are evolved to higher scales according to the perturbative QCD renormalization group equations. All the available observables *e.g.* the proton structure function, $F_2^p(x, Q^2)$, are composed of the candidate PDFs and comparison with the data is made with the help of some statistical estimator such as the global χ^2 ,

$$\chi^2 = \sum_{\text{expt. } i} \sum_{j=1}^{N_e} (\text{Data}_i - \text{Theor}_i) V_{ij}^{-1} (\text{Data}_j - \text{Theor}_j), \quad (1)$$

where the error matrix V_{ij} consists of the statistical and uncorrelated systematic errors, as well as of the correlated systematic errors when available. The parameters in the ansatz are then adjusted and the whole process repeated until a global minimum has been found.

The modern PDF collaborations (CTEQ [1] and references within, MRST [2–4], Alekhin [5, 6], Zeus [7] and H1 [8]) also provide error estimates for the PDF sets. They all rely on some kind of variant of the Hessian method (see e.g. [9] for details), which is based on a Taylor expansion of the global χ^2 around its minimum. When only the leading terms are kept, the displacement of χ^2 can be written in terms of Hessian matrix H_{ij} , which consists of second derivatives of χ^2 with respect to the parameter displacements, evaluated at the minimum. The error estimate for the parameters themselves, or for any quantity that depends on those parameters, can then be obtained in terms of the inverse of the Hessian matrix,

$$(\Delta X)^2 = \Delta\chi^2 \sum_{i,j} \frac{\partial X}{\partial y_i} (H^{-1})_{ij} \frac{\partial X}{\partial y_j}. \quad (2)$$

For details of PDF uncertainty studies see e.g. Refs. [10, 11].

The global analysis combined with Hessian error estimation is a powerful method, allowing for both extrapolation outside the kinematical range of the data and extension to multivariable cases, such as nuclear PDFs (nPDFs) [12–15]. In principle, when more data become available, the method could also be applied to Generalized Parton Distributions (GPDs), for which only model-dependent [16] or semi model-dependent [17, 18] solutions presently exist.

However, there are uncertainties related to the method itself, that are difficult to quantify, but may turn out to have a large effect. Choosing global χ^2 as a statistical estimator may not be adequate since the minimum of the global fit may not correspond to a minima of the individual data sets, and as a result the definition of $\Delta\chi^2$ may be ambiguous. Estimates for the current major global analyses are that $\Delta\chi^2 = 50 - 100$ is needed to obtain a $\sim 90\%$ confidence interval [1, 2]. In principle this problem could be avoided by using the Lagrange multiplier method (see e.g. [19]), which does not assume quadratic behaviour for the errors around the minimum, instead of the Hessian method,

but this is computationally more expensive solution. Introducing a functional form at the initial scale necessarily introduces a parametrization dependence bias and theoretical assumptions behind the fits, such as s , \bar{s} , c quark content, details of the scale evolution (e.g. higher order perturbative corrections, large/small x resummation), higher twists etc. as well as the data selection and treatment, e.g. kinematical cuts, all reflect into the final result of the analysis. Also, there may be systematical bias introduced by the optimization algorithm. The differences between the current global PDF sets tend to be larger than the estimated uncertainties [20], and these differences again translate to the predictions for the LHC observables, such as Higgs [21] or W^\pm and Z production cross sections [1].

A new, fresh approach to the PDF fitting has recently been proposed by NNPDF collaboration [22,23] who have replaced a typical functional form ansatz with a more complex standard neural network (NN) solution and the Hessian method with Monte Carlo sampling of the data (see the references within [23] for the nonsinglet PDF fit and the details of the Monte Carlo sampling).

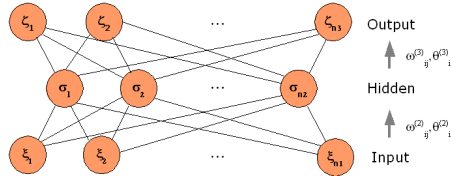


Figure 1: Schematic diagram of a feed-forward neural network, from [24].

Neural network can be described as a computing solution that consists of interconnected processing elements, neurons, that work together to produce an output function. In a typical feed-forward NN (see Fig. 1) the output is given by the neurons in the last layer, as a non-linear function of the output of all neurons in the previous layer, which in turn is a function of the output of all neurons in the previous layer, and so on, starting from the first layer, which receives the input. For a NN with L layers and n_l neurons in each layer, the total number of the parameters is $\sum_{l=1}^{L-1} (n_l n_{l+1} + n_{l+1})$.

In the beginning of the NNPDF fitting procedure a Monte Carlo sample of replicas of the experimental data is generated by jittering the central values of the data withing their errorbars using univariate Gaussian (or some other distribution if desired) random numbers for each independent error source. The number of the replicas is made so large that the Monte Carlo set of replicas models faithfully the probability distribution of the original data. For each replica a Genetic Algorithm (GA) fit is performed by first setting the NN parameters for each parton flavour to be fitted randomly, then making clones of the set of parameters, and mutating each of them randomly (multiple mutations). After scale evolution the comparison with the data is performed for all the clones, and the best clones are selected for a source of new clones, and the process repeated until the minimum for the χ^2 has been found. Overfitting of the data is prevented by using only part of the data in the minimizing procedure, and using the other part to monitor the behaviour of the χ^2 . When fitting PDFs one thus ends up with N_{rep} PDF sets, each initial scale parton distribution parametrized by a different NN. The quality of the global fit is then given by the χ^2 computed from the averages over the sample of trained neural networks. The mean value of the parton distribution at the starting scale for a given value of x is found by averaging over the replicas, and the uncertainty on this value is the variance of the values given by the replicas.

The NNPDF method circumvents the problem of choosing a suitable $\Delta\chi^2$, and it relies on GA which works on a population of solutions for each MC replica, thus having a lowered possibility of getting trapped in local minima. NN parametrizations are also highly complex, with large number of parameters, and thus unbiased compared to the ansatze used in global fits. The estimated uncertainties for NNPDF fits are larger than those of global fits, possibly indicating that the global fit uncertainties may have been underestimated. It should, however, be pointed out that the MC sampling of the data is not not tied to use of NNs, and it thus remains undetermined whether the large uncertainties would persist if the MC sampling was used with a fixed functional form. The complexity of NN results may also induce problems, especially when used in a purely automated fitting procedure. Since the effect of modifying individual NN parameters is unknown, the result may exhibit

strange or unwanted behaviour in the extrapolation region, or in between the data points if the data is sparse. In such a case, and in a case of incompatible data, the overfitting method is also unsafe to use. Implementation of information not given directly by the data, such as nonperturbative models, lattice calculations or knowledge from prior work in general, is also difficult in this approach.

A possible method of estimating the PDF uncertainties could also be provided by Bayesian statistical analysis, as preliminarily studied in [25, 26] and explained in [27], in which the errors for the PDF parameters, or for an observable constructed from the PDFs, are first encapsulated in prior probabilities for an enlarged set of model parameters, and posterior distributions are obtained using computational tools such as Markov Chain Monte Carlo. Similar to NNPDF approach, this method allows for an inclusion of non-Gaussian systematic errors for the data.

In this introductory paper we propose a new method which relies on the use of Self-Organizing Maps (SOMs), a subtype of neural network. The idea of our method is to create means for introducing “Researcher Insight” instead of “Theoretical bias”. In other words, we want to give up fully automated fitting procedure and eventually develop an interactive fitting program which would allow us to “take the best of both worlds”, to combine the best features of both the standard functional form approach and the neural network approach. In this first step, we solely concentrate on single variable functions, free proton PDFs, but discuss the extension of the model to multivariable cases. In Section 2 we describe the general features of the SOMs, in Sections 3 and 4 we present two PDF fitting algorithms relying on the use of SOMs and finally in Section 5 we envision the possibilities the SOM method has to offer.

2 Self-Organizing Maps

The SOM is a visualization algorithm which attempts to represent all the available observations with optimal accuracy using a restricted set of models. The SOM was developed by T. Kohonen in the early 1980’s ([28], see also [29]) to model biological brain functions, but has since then developed

into a powerful computational approach on its own right. Many fields of science, such as statistics, signal processing, control theory, financial analyses, experimental physics, chemistry and medicine, have adopted the SOM as a standard analytical tool. SOMs have been applied to texture discrimination, classification/pattern recognition, motion detection, genetic activity mapping, drug discovery, cloud classification, and speech recognition, among others. Also, a new application area is organization of very large document collections. However, applications in particle physics have been scarce so far, and mostly directed to improving the algorithms for background event rejection [30–32].

SOM consists of nodes, map cells, which are all assigned spatial coordinates, and the topology of the map is determined by a chosen distance metric M_{map} . Each cell i contains a map vector V_i , that is isomorphic to the data samples used for training of the neural network. In the following we will concentrate on a 2-dimensional rectangular lattice for simplicity. A natural choice for the topology is then $L_1(x, y) = \sum_{i=1}^2 |x_i - y_i|$, which also has been proved [33] to be an ideal choice for high-dimensional data, such as PDFs in our case.

The implementation of SOMs proceeds in three stages: 1) initialization of the SOM, 2) training of the SOM and 3) associating the data samples with a trained map, i.e. clustering. During the initialization the map vectors are chosen such that each cell is set to contain an arbitrarily selected sample of either the actual data to be clustered, or anything isomorphic to them (see Fig. 2 for an example). The actual training data samples, which may be e.g. subset or the whole set of the actual data, are then associated with map vectors by minimizing a similarity metric M_{data} . We choose $M_{\text{data}} = L_1$. The map vector each data sample becomes matched against, is then the most similar one to the data sample among all the other map vectors. It may happen that some map vectors do not have any samples associated with them, and some may actually have many.

During the training the map vectors are updated by averaging them with the data samples that fell into the cells within a given decreasing neighbourhood, see Fig. 3. This type of training which is based on rewarding the winning node to become more like data, is called *competitive learning*. The initial value of a map vector V_i at SOM cell i then changes during the course of

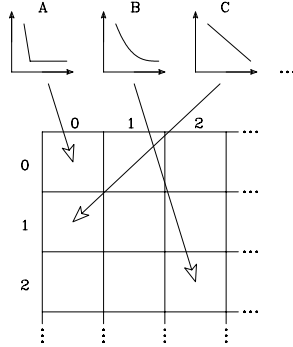


Figure 2: A 2D grid SOM which cells get randomly associated with the type of data samples we would like to study, such as nonsinglet PDFs or observables. At this stage each cell gets associated with only one curve, the map vector.

training as

$$V_i(t + 1) = V_i(t) (1 - w(t) N_{j,i}(t)) + S_j(t) w(t) N_{j,i}(t) \quad (3)$$

where now $V_i(t + 1)$ is the contents of the SOM cell i after the data sample S_j has been presented on the map. The neighbourhood, the radius, within which the map vectors are updated is given by the function $N_{j,i}(t)$, centered on the winner cell j . Thus even the map vectors in those cells that didn't find a matching data sample are adjusted, rewarded, to become more like data. Typically $N_{j,i}(t) = e^{-M_{map}(j,i)^2/r(t)}$, where $r(t)$ is a monotonously decreasing radius sequence. In the beginning of the training the neighbourhood may contain the whole map and in the end it just consists of the cell itself. Moreover, the updating is also controlled by $w(t)$, which is a monotonously decreasing weight sequence in the range $[0, 1]$.

As the training proceeds the neighbourhood function eventually causes the data samples to be placed on a certain region of the map, where the neighbouring map vectors are becoming increasingly similar to each other, and the weight sequence $w(t)$ furthermore finetunes their position.

In the end on a properly trained SOM, cells that are topologically close to each other will have map vectors which are similar to each other. In the final phase the actual data is matched against the map vectors of the trained map, and thus get distributed on the map according to the feature that was used

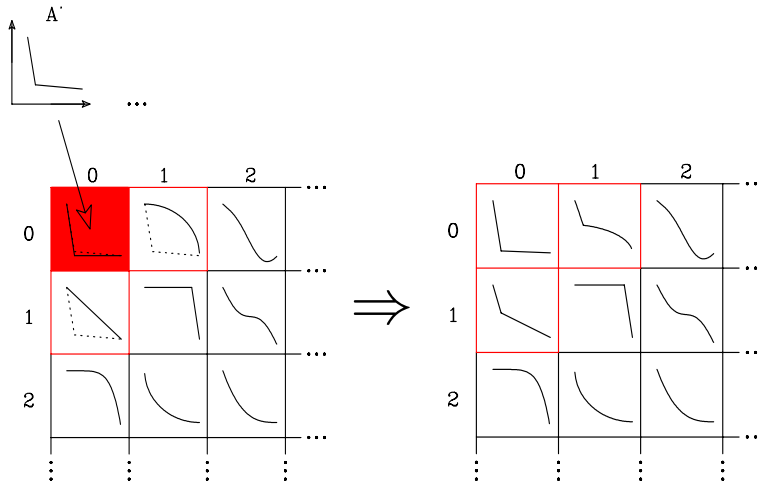


Figure 3: (Colour online) Each data sample S_i is associated with the one map vector V_i it is most similar to. As a reward for the match, the winning map vector, as well as its neighbouring map vectors, get averaged with the data associated with the winning cell.

as M_{data} . Clusters with similar data now emerge as a result of *unsupervised learning*.

For example, a map containing RGB colour triplets would initially have colours randomly scattered around it, but during the course of training it would evolve into patches of colour which smoothly blend with each other, see Fig. 4. This local similarity property is the feature that makes SOM suitable for visualization purposes, thus facilitating user interaction with the data. Since each map vector now represent a class of similar objects, the SOM is an ideal tool to visualize high-dimensional data, by projecting it onto a low-dimensional map clustered according to some desired similar feature. SOMs, however, also have disadvantages. Each SOM, though identical in size and shape and containing same type of data, is different. The clusters may also split in such a way that similar type of data can be found in several different places on the map. We are not aware of any mathematical or computational means of detecting if and when the map is fully trained, and whether there occurs splitting or not, other than actually computing the

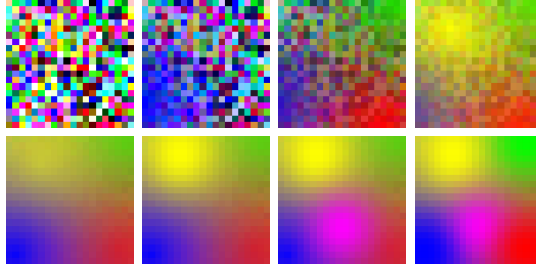


Figure 4: (Colour online) SOM containing RGB colour triplets getting trained. Adapted from Ref. [34]

similarities between the neighbouring cells and studying them.

In this work we use the so-called batch-version of the training, in which all the training data samples are matched against the map vectors before the training begins. The map vectors are then averaged with all the training samples within the neighbourhood radius simultaneously. The procedure is repeated N_{step} (free parameter to choose) times such that in every training step the *same* set of training data samples is associated with the evolving map and in Eq.(3) t now counts training steps. When the map is trained, the actual data is finally matched against the map vectors. In our study our training data are always going to be the whole data we want to cluster, and the last training step is thus the clustering stage. The benefit of the batch training compared to the incremental training, described earlier, is that the training is independent of the order in which the training samples are introduced on the map.

3 MIXPDF algorithm

In this approach our aim is to both i) to be able to study the properties of the PDFs in a model independent way and yet ii) to be able to implement knowledge from the prior works on PDFs, and ultimately iii) to be able to guide the fitting procedure interactively with the help of SOM properties.

At this stage it is important to distinguish between the experimental data

and the training data of the SOM. When we are referring to measured data used in the PDF fitting, such as F_2 data, we always call it experimental data. The SOM training data in this study is going to be a collection of candidate PDF sets, produced by us, or something composed of them. A PDF set in the following will always mean a set of 8 curves, one for each independent parton flavour $f = (g, u_v, d_v, \bar{u}, \bar{d}, s = \bar{s}, c = \bar{c}$ and $b = \bar{b}$ in this simplified introductory study), that are properly normalized such that

$$\sum_f \int_0^1 dx x f_{f/p}(x, Q^2) = 1, \quad (4)$$

and conserve baryon number and charge

$$\int_0^1 dx f_{u_v/p}(x, Q^2) = 2, \quad \int_0^1 dx f_{d_v/p}(x, Q^2) = 1. \quad (5)$$

In order to proceed we have to decide how to create our candidate PDF sets, decide the details of the SOMs, details of the actual fitting algorithm, experimental data selection and details of the scale evolution.

In this introductory paper our aim is not to provide a finalised SOMPDF set, but rather to explore the possibilities and restrictions of the method we are proposing. Therefore we refrain from using “all the possible experimental data” as used in global analyses, but concentrate on DIS structure function data from H1 [35], BCDMS [36, 37] and Zeus [38], which we use without additional kinematical cuts or normalization factors (except rejecting the data points below our initial scale). The parameters for the DGLAP scale evolution were chosen to be those of CTEQ6 (CTEQ6L1 for lowest order (LO)) [39], the initial scale being $Q_0 = 1.3$ GeV. In next-to-leading order (NLO) case the evolution code was taken from [40] (QCDNUM17 beta release).

We will start now with a simple pedagogical example, which we call MIXPDF algorithm, where we use some of the existing PDF sets as material for new candidate PDFs. At first, we will choose CTEQ6 [39], CTEQ5 [41], MRST02 [2, 42], Alekhin [5] and GRV98 [43] sets and construct new PDF sets from them such that at the initial scale each parton flavour in the range $x = [10^{-5}, 1]$ is randomly selected from one of these five sets (we set the heavy flavours to be zero below their mass thresholds). The sumrules on this new

set are then imposed such that the original normalization of u_v and d_v are preserved, but the rest of the flavours are scaled together so that Eq.(4) is fulfilled. In this study we accept the <few% normalization error which results from the fact that our x -range is not $x = [0, 1]$. From now on we call these type of PDF sets *database* PDFs. We randomly initialize a small 5×5 map with these candidate database PDFs, such that each map vector V_i consists of the PDF set itself, and of the observables $F_2^p(x, Q_0^2)$ derived from it. Next we train the map with $N_{\text{step}} = 5$ batch-training steps with training data that consists of 100 database PDFs plus 5 original “mother” PDF sets, which we will call *init* PDFs from now on. We choose the similarity criterion to be the similarity of observables $F_2^p(x, Q^2)$ with $M_{\text{data}} = L_1$. The similarity is tested at a number of x -values (equidistant in logarithmic scale up to $x \sim 0.2$, and equidistant in linear scale above that) both at the initial scale and at all the evolved scales where experimental data exist. On every training, after the matching, all the observables (PDFs) of the map vectors get averaged with the observables (PDFs, flavor by flavor) matched within the neighbourhood according to Eq. (3). The resulting new averaged map vector PDFs are rescaled again (such that u_v and d_v are scaled first) to obey the sumrules. From now on we will call these type of PDF sets *map* PDFs. The map PDFs are evolved and the observables at every experimental data scale are computed and compared for similarity with the observables from the training PDFs.

After the training we have a map with 25 map PDFs and the same 105 PDF sets we used to train the map. The resulting LO SOM is shown in Fig. 5, with just $F_2^p(x, Q_0^2)$'s of each cell shown for clarity. The red curves in the figure are the map F2's constructed from the map PDFs, black curves are the database F2's and green curves are the init F2's constructed from the init PDFs (CTEQ6, CTEQ5, MRST02, Alekhin and GRV98 parametrizations). It is obviously difficult to judge visually just by looking at the curves whether the map is good and fully trained. One hint about possible ordering may be provided by the fact that the shape of the F_2^p curve must correlate with the χ^2/N against the experimental data. The distribution of the χ^2/N values (no correlated systematic errors are taken into account for simplicity) of the map PDFs, shown in each cell, does indeed seem somewhat organized.

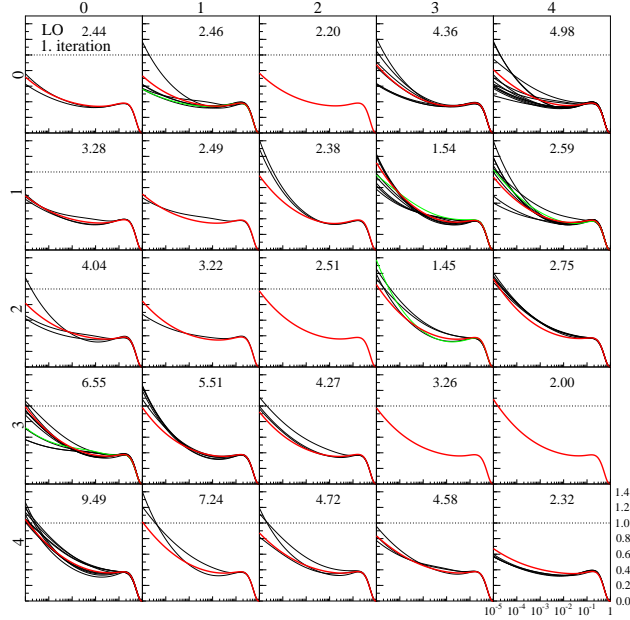


Figure 5: (Colour online) Trained 1. iteration LO map. Red curves are map F_2^p 's, green curves init F_2^p 's and black curves rest of the database F_2^p 's. The number in each cell is the χ^2/N of the map PDF.

Table 1 lists the χ^2/N values the original init PDFs obtain within the MIX-PDF framework described above. Comparison of these values with the values in Fig. 5 reveals that some of the map PDFs, as also some of the database PDFs, have gained a χ^2/N comparable to or better than that of the init PDFs.

Inspired by the progress, we start a second fitting *iteration* by selecting the 5 best PDF sets from the 25+5+100 PDF sets of the first iteration as our new init PDFs (which are now properly normalized after the first iteration) to generate database PDFs for a whole new SOM. Since the best PDF candidate from the first iteration is matched on this new map as an unmodified init PDF, it is guaranteed that the χ^2/N as a function of the iteration either decreases or remains the same. We keep repeating the iterations until the χ^2/N saturates. Fig. 6 (Case 1) shows the χ^2/N as a function of iterations for the best PDF on the trained map, for the worst PDF on the map and for

PDF [‡]	LO χ^2/N	NLO χ^2/N
Alekhin	3.34	29.1
CTEQ6	1.67	2.02
CTEQ5	3.25	6.48
CTEQ4	2.23	2.41
MRST02	2.24	1.89
GRV98	8.47	9.58

Table 1: χ^2/N for different MIXPDF input PDF sets against all the datasets used (H1, ZEUS, BCDMS, N=709).

the worst of the 5 PDFs selected for the subsequent iteration as an init PDF. The final χ^2/N of these runs are listed in Table 2 (first row) as Case 1 and Fig. 7 shows these results (black solid line), together with original starting sets at the initial scale (note the different scaling for gluons in LO and in NLO figures). For 10 repeated LO runs we obtain $\bar{\chi}^2/N=1.208$ and $\sigma=0.029$. Let us now analyze in more detail how the optimization proceeds. Figs. 8,9 show the LO maps also for the 2. and 3. iterations. On the first iteration the init PDFs, the shapes of which were taken from existing parametrizations, fall in the cells (0,1) (CTEQ5), (1,3) (Alekhin), (1,4) (MRST02), (2,3) (CTEQ6) and (3,0) (GRV98), so the modern sets, Alekhin, MRST02 and CTEQ6, group close to each other, i.e. the shapes of the observables they produce are very similar, as expected. The best 5 PDFs selected as the 2. iteration init PDFs also come from this neighbourhood, 3 of them from the cell (1,3) and the other 2 from the cell (2,3). Two of these selected sets are map PDFs, two are database PDFs and also the original init PDF CTEQ6 survived for the 2. iteration.

At the end of the 2. iteration the init PDFs, which originated from the neighbouring cells, are scattered in the cells (0,1), (0,3), (1,0) (CTEQ6),

[‡]These are the χ^2/N for the initial scale PDF sets taken from the quoted parametrizations and evolved with CTEQ6 DGLAP settings, the heavy flavours were set to be zero below their mass thresholds, no kinematical cuts or normalization factors for the experimental data were imposed, and no correlated systematic errors of the data were used to compute the χ^2/N . We do not claim these values to describe the quality of the quoted PDF sets.

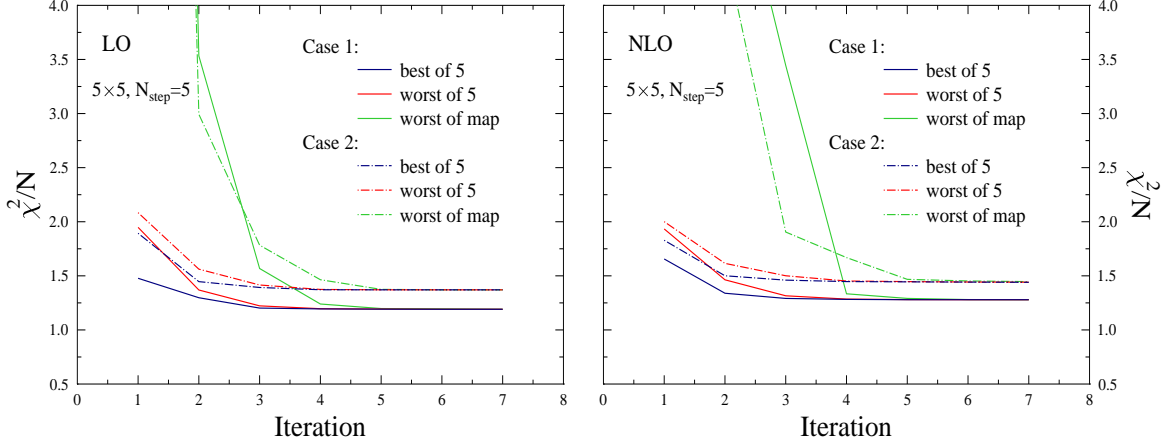


Figure 6: (Colour online) χ^2/N of the MIXPDF runs as a function of the iteration.

(2,2) and (2,3) and the best 5 PDFs produced during this iteration are in the cells (4,1) (database PDF), (4,0) (map PDF), (3,2) (map PDF), (2,2) (database PDF) and (3,0) (map PDF).

After the 3. iteration the above best 5 PDFs of 2. iteration are in the cells (2,0), (3,1), (0,2), (0,4) and (3,2) and the new best 5 PDFs produced are all map PDFs with 4 of them in neighbouring cell pairs.

Map PDFs provide complicated linear combinations of the database PDFs and obviously play an important role in the algorithm. The size of the map dictates how much the neighbouring map vectors differ from each other. Since the PDFs in the same cell are not required to be similar, only the observables constructed from them are, a cell or a neighbourhood may in principle contain a spread of PDFs with a spread of χ^2/N 's. However, since our selection criteria for the init PDFs was based on the best χ^2/N only, it is inevitable that the observables on the map become increasingly similar as the iterations go by, and the χ^2/N flattens very fast as can be seen from Fig. 6. As a consequence we quickly lose the variety in the shapes of the PDFs as the iterations proceed, and on the final iteration all the PDFs on the map end up being very similar.

SOM	N_{step}	# init	# database	Case	LO χ^2/N	NLO χ^2/N
5x5	5	5	100	1	1.19	1.28
5x5	5	5	100	2	1.37	1.44
5x5	5	10	100	1	1.16	1.25
5x5	5	10	100	2	1.49	1.43
5x5	5	15	100	1	1.16	1.45
5x5	5	20	100	1	1.17	-
5x5	10	10	100	1	1.16	1.30
5x5	40	10	100	1	1.20	-
15x15	5	5	900	1	1.22	-
15x15	5	5	900	2	1.31	-
15x15	5	30	900	1	1.16	1.25
15x15	5	30	900	2	1.25	1.53

Table 2: χ^2/N against all the datasets used (H1, ZEUS, BCDMS) for some selected MIXPDF runs.

The MIXPDF algorithm obviously has several other weaknesses too. Among them are how the result would change if we started with another first iteration PDF selection, and what are the effects of changing the size of the map, number of the database PDFs and init PDF sets and size of N_{step} ? In general, how much the final result depends on the choices that we make during the fitting process?

Let us now study some of these questions a bit. Since we have chosen our evolution settings to be those of CTEQ6's, it necessarily becomes a favoured set (although we don't impose any kinematical cuts on the experimental data). Therefore we performed another LO and NLO runs, with CTEQ6 now replaced with CTEQ4 [44]. The results of these runs are reported in Table 2 (2. row) and in Fig. 6 (χ^2/N) and Fig. 7 (the PDFs) as Case 2. The Case 2 clearly produces worse results. Without an input from CTEQ6 we automatically lose all the low gluons at small- x -type of results in NLO, for example.

Fig. 10 addresses the issue of choosing different N_{step} , for LO Case 1 and Case 2. The solid (dotted) lines show the best (worst) init PDF selected

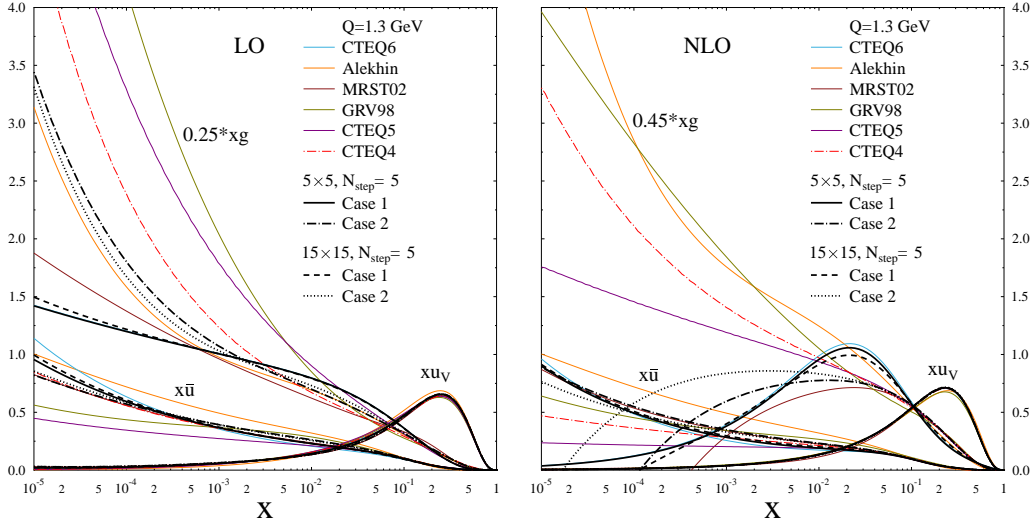


Figure 7: (Colour online) MIXPDF results together with the input PDF sets.

from each iteration for several N_{step} selections. In Case 2 the best results are obtained with small number of training steps, whereas Case 1 does not seem to benefit from a longer SOM training. Keeping the stochastic nature of the process in our minds, we may speculate that the seemingly opposite behaviour for the Case 1 and Case 2 results from the fact that it is more probable to produce a good set of database PDFs in Case 1 than in Case 2. If the database is not so good to begin with, the longer training contaminates all the map PDFs with the low quality part of the database PDFs.

Table 2 also showcases best results from a variety of MIXPDF runs where we have tried different combinations of SOM features. It is interesting to notice that increasing the size of the map and database does not necessarily lead to a better performance. Instead the number of the init PDFs on later iterations (always 5 for the first iteration) seem to be a key factor, it has to be sufficiently large to preserve the variety of database the PDFs but small enough to consist of PDFs with good quality. In our limited space of database candidates ($\sim 6^5 = 7776$ possibilities) the optimal set of variables

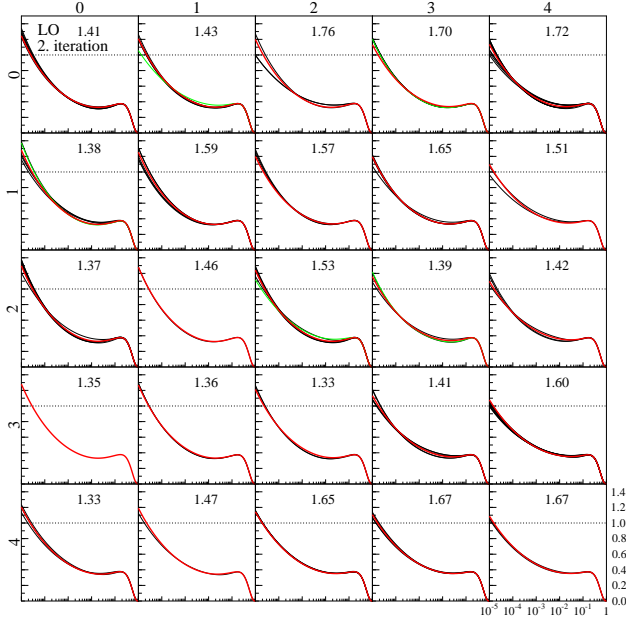


Figure 8: (Colour online) Trained 2. iteration LO map, curves and numbers as in Fig.5.

for the MIXPDF run should not be not impossible to map down.

The method we used to generate the sample data is very simple indeed. The number of all the possible candidate database PDFs is not very large to begin with, so the quality of the final results strongly depends on the quality of the input for the SOM. Since the map PDFs are obtained by averaging with the training samples, and the non-valence flavours are scaled by a common factor when imposing the sumrules, the map PDFs tend to lie in between the init PDFs. Therefore map PDFs with extreme shapes are never produced, and thus never explored by the algorithm.

A method which relies on sampling existing parametrizations on a SOM is inconvenient also because it is not readily applicable to multivariable cases. For the case of the PDFs it is sufficient to have a value for each flavour for a discrete set of x -values, but for a multivariable cases, such as nPDFs, or GPDs the task of keeping track of the grid of values for each flavour in each x for several different values of the additional variables (*e.g.* A and Z

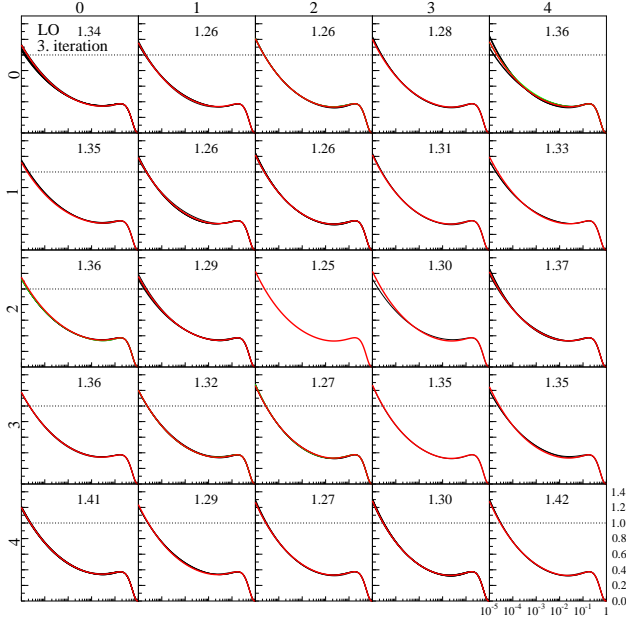


Figure 9: (Colour online) Trained 3. iteration LO map, curves and numbers as in Fig.5.

for nuclei, and the skewness, ξ and the squared 4-momentum transfer, t for GPDs) is computationally expensive. In principle, SOM can keep track of the interrelations of the map vectors, and knowing the parametrization for the init PDFs, it would be possible to construct the parametrization for the map PDFs. That would, however, lead to very complicated parametrizations, and different nPDF, GPD etc. parametrizations are presently not even either measured or defined at the same initial scale.

Despite of its problems, on a more basic level, MIXPDF does have the the desirable feature that it allows us to use SOM as a part of the PDF optimization algorithm in such a way that we cluster our candidate PDFs on the map, and select those PDFs which *i*) minimize a chosen fitness function, e.g. χ^2 , when compared against experimental data, and *ii*) have some desired feature which can be visualized on the map or used as a clustering criterion. Therefore, in the following Section, we keep building on this example.

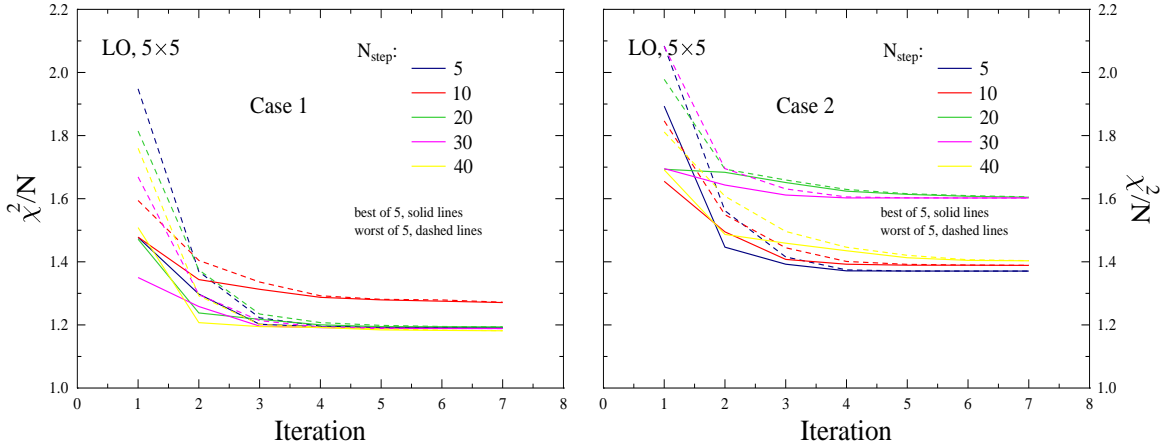


Figure 10: (Colour online) LO χ^2/N for 5×5 SOM runs with different N_{step} .

4 ENVPDF algorithm

Most of the problems with the MIXPDF algorithm originate from the need to be able to generate the database PDFs in an unbiased way as possible, and at the same time to have a variety of PDF candidates available at every stage of the fitting procedure. Yet, one needs to have control over the features of the database PDFs that are created.

To accomplish this, we choose, at variance with the “conventional” PDFs sets or NNPDFs, to give up the functional form of PDFs and rather to rely on purely stochastic methods in generating the initial and training samples of the PDFs. Our choice is a GA-type analysis, in which our parameters are the values of PDFs at the initial scale for each flavour at each value of x where the experimental data exist. To obtain control over the shape of the PDFs we use some of the existing distributions to establish an initial range, or *envelope*, within which we sample the database PDF values.

Again, we use the Case 1 and 2 PDF sets (CTEQ6, CTEQ5, CTEQ4, MRST02, Alekhin and GRV98) as an initialization guideline. We construct our initial PDF generator first to, for each flavour separately, select ran-

domly either the range $[0.5, 1]$, $[1.0, 1.5]$ or $[0.75, 1.25]$ times any of the Case 1 (or 2) PDF set. Compared to MIXPDF algorithm we are thus adding more freedom to the scaling of the database PDFs. Next the initial generators generate values for each x_{data} [§] using uniform, instead of Gaussian, distribution around the existing parametrizations, thus reducing direct bias from them. Gaussian smoothing is applied to the resulting set of points, and the flavours combined to form a PDF set such that the curve is linearly interpolated from the discrete set of generated points.

The candidate PDF sets are then scaled to obey the sumrules as in MIXPDF algorithm. In order to obtain a reasonable selection of PDFs to start with, we reject candidates which have $\chi^2/N > 10$ (computed as in MIXPDF algorithm). To further avoid direct bias from the Case 1 and 2 PDFs, we don't include the init PDFs into the training set for the first iteration as we did in MIXPDF case. For a $N \times N$ SOM we choose the size of the database to be $4N^2$.

During the later iterations we proceed as follows: At the end of each iteration we pick from the trained $N \times N$ SOM $2N$ best PDFs as the init PDFs. These init PDFs are introduced into the training set alongside with the database PDFs, which are now constructed using each of the init PDFs *in turn* as a center for a Gaussian random number generator, which assigns for *all* the flavours for each x a value around that *same* init PDF such that $1 - \sigma$ of the generator is given by the spread of the best PDFs in the topologically nearest neighbouring cells. The object of these generators is thus to refine a good candidate PDF found in the previous iteration by jittering it's values within a range determined by the shape of other good candidate PDFs from the previous iteration. The generated PDFs are then smoothed and scaled to obey the sumrules. Sets with $\chi^2/N > 10$ are always rejected. We learnt from the MIXPDF algorithm that it is important to preserve the variety of the PDF shapes on the map, so we also keep N_{orig} copies of the first iteration generators in our generator mix.

Table 3 lists results from a variety of such runs. The results do not seem

[§]To ensure a reasonable large- x behaviour for the PDFs, we also generate with the same method values for them in a few x -points outside the range of the experimental data. We also require the PDFs, the gluons especially, to be positive for simplicity.

to be very sensitive to the number of SOM training steps, N_{step} , but are highly sensitive to the number of first iteration generators used in subsequent iterations. Although the generators can now in principle produce an infinite number of different PDFs, the algorithm would not be able to radically change the shape of the database PDFs without introducing a random element on the map. Setting $N_{\text{orig}} > 0$ provides, through map PDFs, that element, and keeps the algorithm from getting fixed to a local minimum. The ENVPDF algorithm is now more independent from the initial selection of the PDF sets, Case 1 or 2, than MIXPDF, since no values of *e.g.* the CTEQ6 set in the original generator are ever introduced on the map directly.

SOM	N_{step}	N_{orig}	Case	LO χ^2/N	NLO χ^2/N
5x5	5	2	1	1.04	1.08
5x5	10	2	1	1.10	-
5x5	20	2	1	1.10	-
5x5	30	2	1	1.10	-
5x5	40	2	1	1.08	-
5x5	5	0	1	1.41	-
5x5	20	0	1	1.26	-
5x5	5	2	2	1.14	1.25
5x5	10	2	2	1.12	-
5x5	15	2	2	1.18	-
15x15	5	6	1	1.00	1.07
15x15	5	6	2	1.13	1.18

Table 3: χ^2/N against all the datasets used (H1, ZEUS, BCDMS) for variety of ENVPDF runs.

Fig. 11 shows the χ^2/N as a function of iteration for 5x5 LO and NLO, both Case 1 and Case 2, runs, where $N_{\text{step}} = 5$ and $N_{\text{orig}} = 2$. Clearly the ENVPDF runs take multiple number of iterations for the χ^2/N to level compared to the MIXPDF runs, and they are therefore more costly in time. With the ENVPDF algorithm, however, the χ^2/N keeps on slowly improving even after all the mother PDFs from the same iteration are equally good fits. For a larger 15x15 SOM the number of needed iterations remains as large.

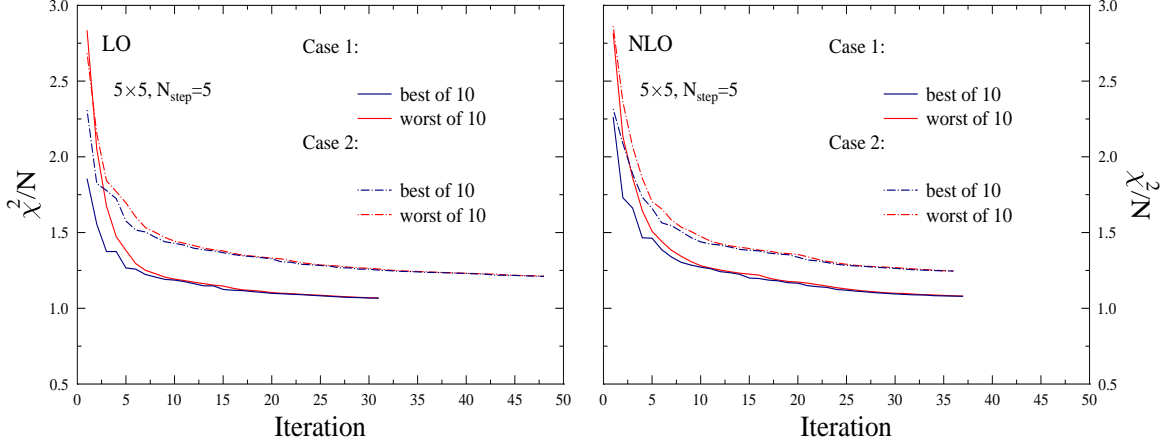


Figure 11: (Colour online) χ^2/N of the ENVPDF runs as a function of the iteration.

Fig. 12 shows some of the Case 1 LO ENVPDF results at the initial scale $Q = 1.3$ GeV (left panel), and evolved up to $Q = 3$ GeV (right panel). The reference curves shown are also evolved as in MIXPDF. Although the initial scale ENVPDF results appear wiggly, they smooth out soon because of the additional well known effect of QCD evolution. In fact, the initial scale curves could be made smoother by applying a stronger Gaussian smoothing, but this is not necessary, as long as the starting scale is below the Q^{\min} of the data. The evolved curves preserve the initially set baryon number scaling within 0.5% and momentum sumrule within 1.5% accuracy. Also, the results obtained from a larger map tend to be smoother since the map PDFs get averaged with a larger number of other PDFs. Studying the relation between the redundant wiggleness of our initial scale PDFs and possible fitting of statistical fluctuations of the experimental data is beyond the scope of this paper. The NLO Case 1 and 2 results are presented in Fig. 13. The trend of the results is clearly the same as in MIXPDF case, CTEQ6 is a favoured set, and especially the PDFs with gluons similar to those of CTEQ6's have good χ^2/N .

We did not study the effect of modifying the width or the shape of the envelope in detail here, but choosing the envelope to be the wider or narrower than $1 - \sigma$ for the Gaussian generate seem to lead both slower and poorer convergence. Also, since we are clustering on the similarity of the observables, the same cell may in theory contain the best PDF of the iteration and PDFs which have χ^2/N as large as 10. Therefore the shape of the envelope should be determined only by the curves with promising shapes.

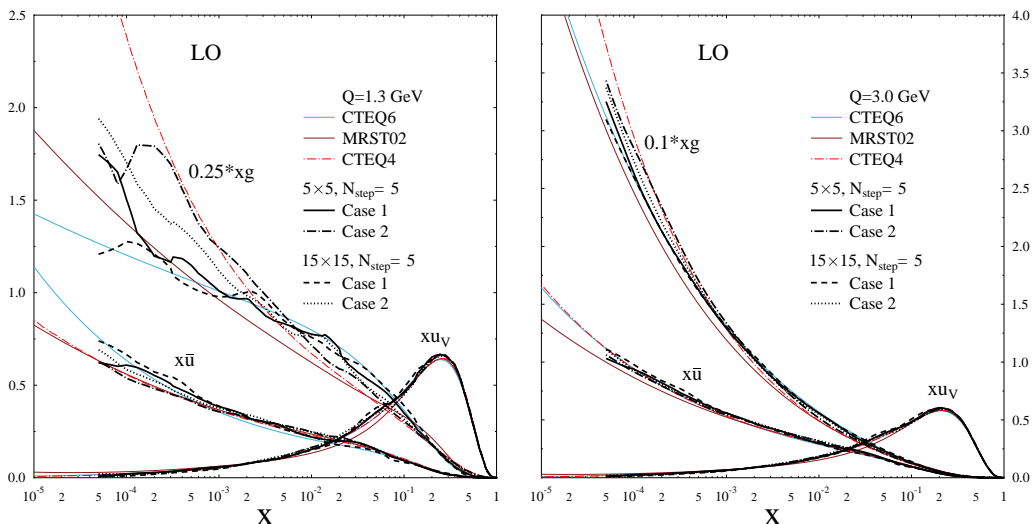


Figure 12: (Colour online) LO ENVPDF results at the initial scale, and at $Q = 3.0$ GeV.

Next we want to study the PDF uncertainty using the unique means the SOMs provide to us even for a case of PDFs without a functional form. Since we have only used DIS data in this introductory study, we are only able to explore the small- x uncertainty for now. Figs. 14 (LO) and 15 (NLO) showcase, besides our best results, the spread of all the initial scale PDFs with $\chi^2/N \leq 1.2$, that were obtained during a 5×5 (left panel) and 15×15 (right panel) SOM run. Since the number of such PDF sets is typically of the order of thousands, we only plot the minimum and maximum of the bundle

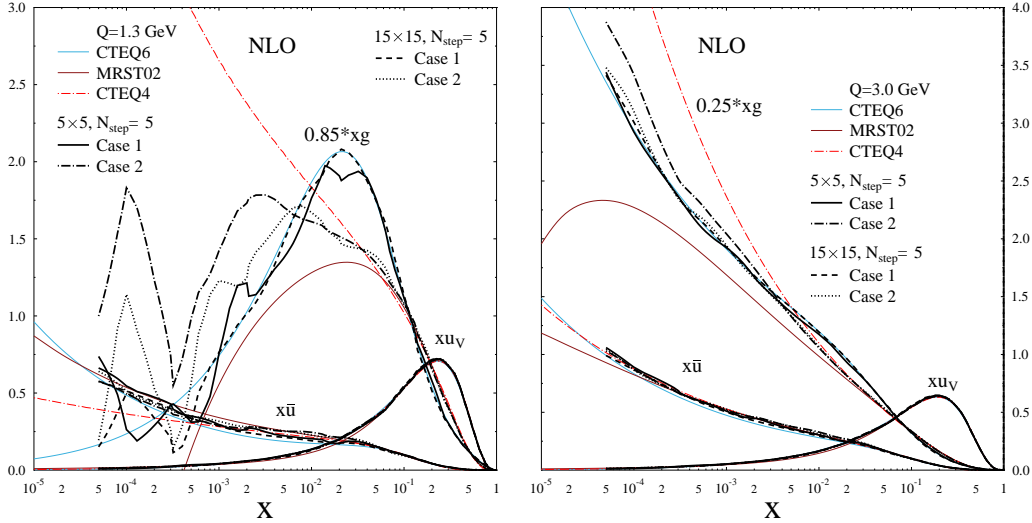


Figure 13: (Colour online) NLO ENVPDF results at the initial scale, and at $Q = 3.0$ GeV.

of curves. Since the total number of experimental datapoints used is ~ 710 , the spread $\Delta\chi^2/N \sim 0.2$ corresponds to a $\Delta\chi^2 \sim 140$. Expectedly, the small- x gluons obtain the largest uncertainty for all the cases we studied. Even though a larger SOM with a larger database might be expected to have more variety in the shapes of the PDFs, the $\chi^2/N \leq 1.2$ spreads of the 5×5 and 15×15 SOMs are more or less equal sized (the apparent differences in sizes at $Q = Q_0$ even out when the curves are evolved). Both maps therefore end up producing the same extreme shapes for the map PDFs although a larger map has more subclasses for them. Remarkably then, a single SOM run can provide a quick uncertainty estimate for a chosen $\Delta\chi^2$ without performing a separate error analysis.

Due to the stochastic nature of the ENVPDF algorithm, we may well also study the combined results from several separate runs. It is especially important to verify the stability of our results, to show that the results are indeed reproducible instead of lucky coincidences. Left panels of Figs 16 (LO) and

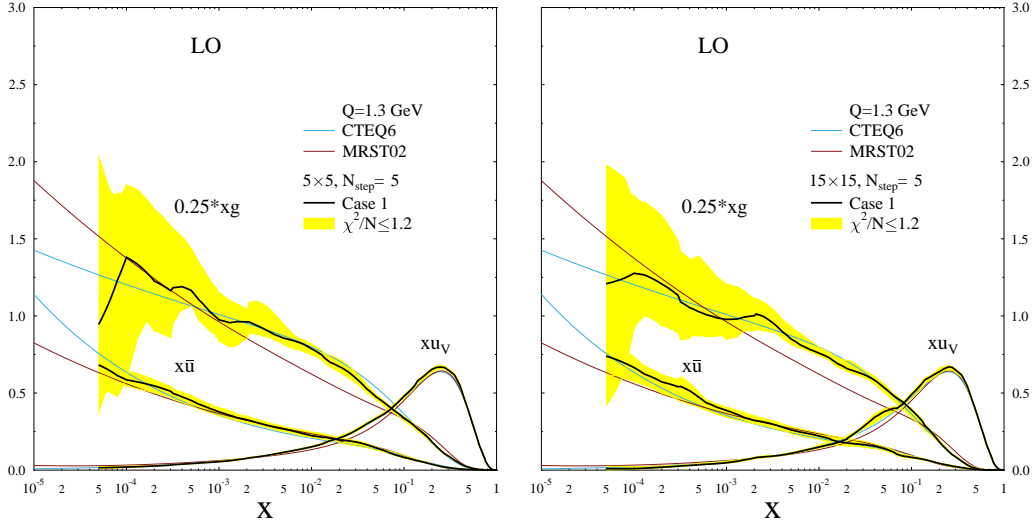


Figure 14: (Colour online) LO ENVPDF best result and the $\chi^2/N \leq 1.2$ spread of results.

17 (NLO) present the best results, and the combined $\chi^2/N \leq 1.2$ spreads for 10 repeated 5×5 , $N_{\text{step}} = 5$ runs at the initial scale. The average χ^2/N and the standard deviation σ for these runs are in LO (NLO) are 1.065 and 0.014 (1.122 and 0.029), corresponding to $\Delta\chi^2 \sim 10$ (20) for LO (NLO). The right panels of the same Figs 16, 17 show the 10 best result curves and the $\chi^2/N \leq 1.2$ spreads evolved up to $Q = 3.0$ GeV. Clearly the seemingly large difference between the small- x gluon results at the initial scale is not statistically significant, but smooths out when gluons are evolved. Thus the initial scale wiggleness of the PDFs is mainly only a residual effect from our method of generating them and not linked to the overtraining of the SOM, and we refrain from studying cases where stronger initial scale smoothing is applied. Therefore our simple method of producing the candidate PDFs by jittering random numbers inside a predetermined envelope is surprisingly stable when used together with a complicated PDF processing that SOMs provide.

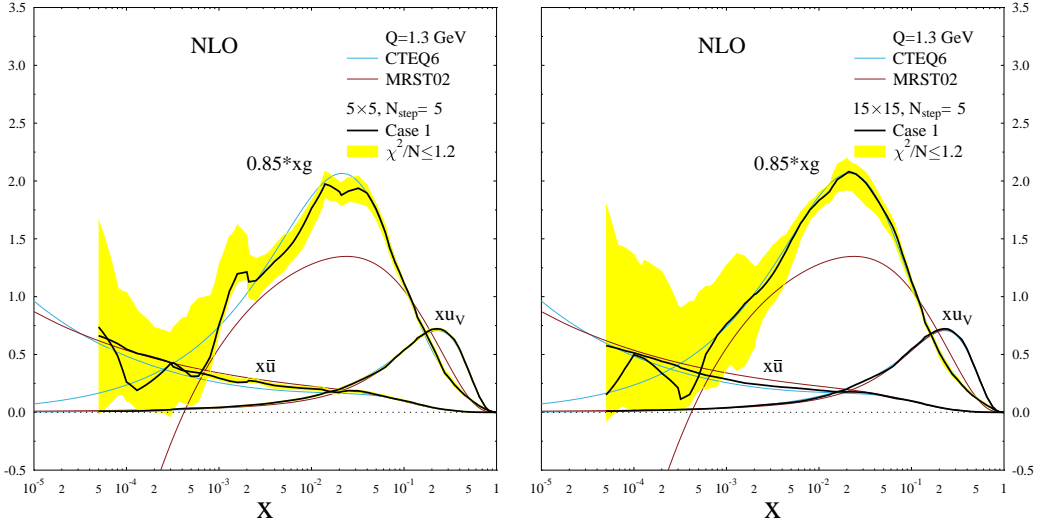


Figure 15: (Colour online) NLO ENVPDF best result and the $\chi^2/N \leq 1.2$ spread of results.

5 Future of the SOMPDFs

So far we have shown a relatively straightforward method of obtaining stochastically generated, parameter-free, PDFs, with an uncertainty estimate for a desired $\Delta\chi^2$. On every iteration using our competitive learning algorithm, the selection of the winning PDFs was based on the χ^2/N alone, and the fitting procedure was fully automated. In our MIXPDF algorithm the SOMs were used merely as a tool to create new combinations, map PDFs, of our input database. The ENVPDF algorithm also used the topology of the map to determine the shape of the envelope, within which we sampled the database PDFs.

We reiterate that our initial study was aimed at observing and recording the behavior of the SOM as an optimization tool. Many of the features of our results could not in fact be predicted based on general assumptions. The proposed method can be extended much further than that. The automated version of the algorithm could be set to sample a vector consisting of PDF

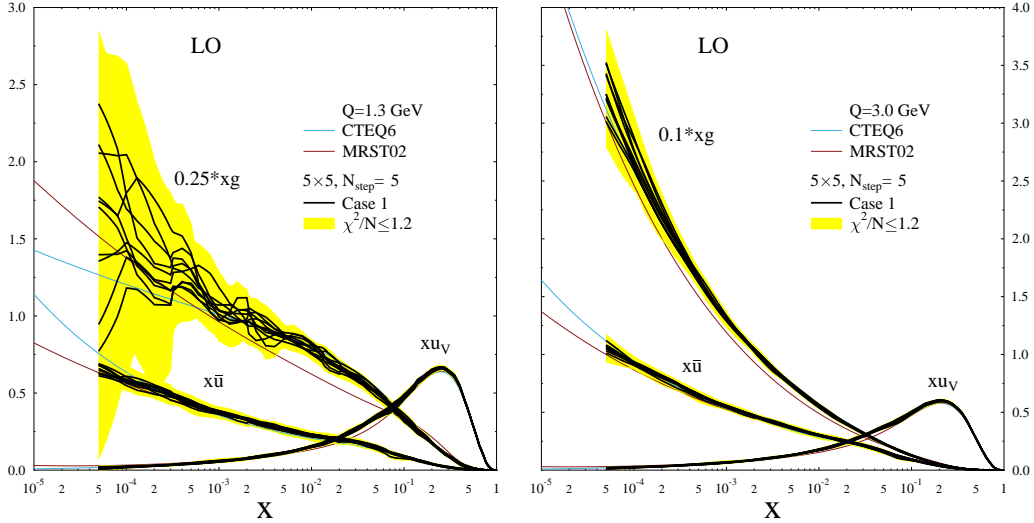


Figure 16: (Colour online) LO ENVPDF best results and the $\chi^2/N \leq 1.2$ spreads of results from 10 separate runs.

parameters, instead of values of PDFs in each value of x of the data. That would lead to smooth, continuous type of solutions, either along the lines of global analyses, or NNPDFs using N SOMs for N Monte-Carlo sampled replicas of the data. Since the solution would be required to stay within an envelope of selected width and shape given by the map, no restrictions for the parameters themselves would be required. For such a method, all the existing error estimates, besides an uncertainty band produced by the map, would be applicable as well.

What ultimately sets the SOM method apart from the standard global analyses or NNPDF method, however, are the clustering and visualization possibilities that it offers. Instead of setting $M_{\text{data}} = L_1$ and clustering according to the similarity of the observables, it is possible to set the clustering criteria to be anything that can be mathematically quantified, e.g. the shape of the gluons or the large- x behaviour of the PDFs. The desired feature of the PDFs can then be projected out from the SOM. Moreover, by combining the

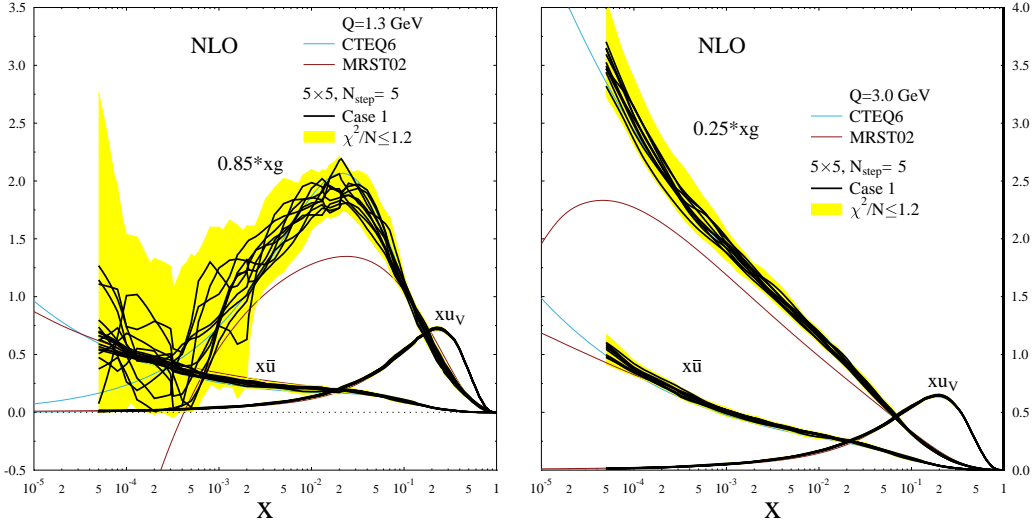


Figure 17: (Colour online) NLO ENVPDF best results and the $\chi^2/N \leq 1.2$ spreads of results from 10 separate runs.

method with an interactive graphic user interface (GUI), it would be possible to change and control the shape and the width of the envelope as the minimization proceeds, to guide the process by applying researcher insight at various stages of the process. Furthermore, the uncertainty band produced by the SOM as the run proceeds, could help the user to make decisions about the next steps of the minimization. With GUI it would be e.g. possible to constrain the extrapolation of the NN generated PDFs outside the x -range of the data without explicitly introducing terms to ensure the correct small- and large- x behaviour as in NNPDF method (see Eq.(87) in [23]). The selection of the best PDF candidates for the subsequent iteration could then be made based on the user's preferences instead of solely based on the χ^2/N . That kind of method in turn could be extended to multivariable cases such as nPDFs and even GPDs and other not so well-known cases, where the data is too sparse for stochastically generated, parameter-free, PDFs. Generally, any PDF fitting method involves a large number of *flexible points*

“opportunities for adapting and fine tuning”, which act as a source for both systematical and theoretical bias when fixed. Obvious optimization method independent sources of theoretical bias are the various parameters of the DGLAP equations, inclusion of extra sources of Q^2 -dependence beyond DGLAP-type evolution and the data selection, affecting the coverage of different kinematical regions. SOMs themselves, and different SOMPDF algorithm variations naturally also introduce flexible points of their own. We explored a little about the effects of choosing the size of the SOM and the number of the batch training steps N_{step} . There are also plenty of other SOM properties that can be modified, such as the shape of the SOM itself. We chose to use a rectangular lattice, but generally the SOM can take any shape desired. For demanding visualization purposes a hexagonal shape is an excellent choice, since the meaning of the nearest neighbours is better defined.

The SOMPDF method, supplemented with the use of a GUI, will allow us to both qualitatively and quantitatively study the flexible points involved in the PDFs fitting. More complex hadronic matrix elements, such as the ones defining the GPDs, are natural candidates for future studies of cases where the experimental data are not numerous enough to allow for a model independent fitting, and the guidance and intuition of the user is therefore irreplaceable. The method we are proposing is extremely open for user interaction, and the possibilities of such a method are widely unexplored.

Acknowledgements

We thank David Brogan for helping us to start this project. This work was financially supported by the US National Science Foundation grant no.0426971. HH was also supported by the U.S. Department of Energy, grant no. DE-FG02-87ER40371. SL is supported by the U.S. Department of Energy, grant no. DE-FG02-01ER41200.

References

- [1] P. M. Nadolsky *et al.*, arXiv:0802.0007 [hep-ph].
- [2] A. D. Martin, R. G. Roberts, W. J. Stirling and R. S. Thorne, Eur. Phys. J. C **23** (2002) 73 [arXiv:hep-ph/0110215].
- [3] A. D. Martin, R. G. Roberts, W. J. Stirling and R. S. Thorne, Phys. Lett. B **604** (2004) 61 [arXiv:hep-ph/0410230].
- [4] A. D. Martin, W. J. Stirling, R. S. Thorne and G. Watt, Phys. Lett. B **652** (2007) 292 [arXiv:0706.0459 [hep-ph]].
- [5] S. Alekhin, Phys. Rev. D **68** (2003) 014002 [arXiv:hep-ph/0211096].
- [6] S. Alekhin, K. Melnikov and F. Petriello, Phys. Rev. D **74** (2006) 054033 [arXiv:hep-ph/0606237].
- [7] S. Chekanov *et al.* [ZEUS Collaboration], Eur. Phys. J. C **42** (2005) 1 [arXiv:hep-ph/0503274].
- [8] C. Adloff *et al.* [H1 Collaboration], Eur. Phys. J. C **30** (2003) 1 [arXiv:hep-ex/0304003].
- [9] J. Pumplin *et al.*, Phys. Rev. D **65** (2002) 014013 [arXiv:hep-ph/0101032].
- [10] A. D. Martin, R. G. Roberts, W. J. Stirling and R. S. Thorne, Eur. Phys. J. C **35** (2004) 325 [arXiv:hep-ph/0308087].
- [11] A. D. Martin, R. G. Roberts, W. J. Stirling and R. S. Thorne, Eur. Phys. J. C **28** (2003) 455 [arXiv:hep-ph/0211080].
- [12] K. J. Eskola, H. Paukkunen and C. A. Salgado, JHEP **0807** (2008) 102 [arXiv:0802.0139 [hep-ph]].

- [13] K. J. Eskola, V. J. Kolhinen, H. Paukkunen and C. A. Salgado, JHEP **0705** (2007) 002 [arXiv:hep-ph/0703104].
- [14] M. Hirai, S. Kumano and T. H. Nagai, Phys. Rev. C **70** (2004) 044905 [arXiv:hep-ph/0404093].
- [15] M. Hirai, S. Kumano and T. H. Nagai, Phys. Rev. C **76** (2007) 065207 [arXiv:0709.3038 [hep-ph]].
- [16] M. Vanderhaeghen, P. A. M. Guichon and M. Guidal, Phys. Rev. D **60** (1999) 094017 [arXiv:hep-ph/9905372].
- [17] S. Ahmad, H. Honkanen, S. Liuti and S. K. Taneja, Phys. Rev. D **75** (2007) 094003 [arXiv:hep-ph/0611046].
- [18] S. Ahmad, H. Honkanen, S. Liuti and S. K. Taneja, arXiv:0708.0268 [hep-ph].
- [19] D. Stump *et al.*, Phys. Rev. D **65** (2002) 014012 [arXiv:hep-ph/0101051].
- [20] J. Pumplin, AIP Conf. Proc. **792**, 50 (2005) [arXiv:hep-ph/0507093].
- [21] A. Djouadi and S. Ferrag, Phys. Lett. B **586** (2004) 345 [arXiv:hep-ph/0310209].
- [22] M. Ubiali, arXiv:0809.3716 [hep-ph].
- [23] R. D. Ball *et al.*, arXiv:0808.1231 [hep-ph].
- [24] L. Del Debbio, S. Forte, J. I. Latorre, A. Piccione and J. Rojo [NNPDF Collaboration], JHEP **0703** (2007) 039 [arXiv:hep-ph/0701127].
- [25] W. T. Giele, S. A. Keller and D. A. Kosower, arXiv:hep-ph/0104052.
- [26] G. Cowan, *Prepared for 14th International Workshop on Deep Inelastic Scattering (DIS 2006), Tsukuba, Japan, 20-24 Apr 2006*

- [27] G. D'Agostini, "*Bayesian Reasoning in Data Analysis: A Critical Introduction*", World Scientific Publishing, Singapore (2003).
- [28] T. Kohonen, *Self-organizing Maps*, Third Edition, Springer (2001).
- [29] <http://www.cis.hut.fi/projects/somtoolbox>
- [30] J. S. Lange, H. Freiesleben and P. Hermanowski, Nucl. Instrum. Meth. A **389** (1997) 214.
- [31] K. H. Becks, J. Drees, U. Flagmeyer and U. Muller, Nucl. Instrum. Meth. A **426** (1999) 599.
- [32] J. S. Lange, C. Fukunaga, M. Tanaka and A. Bozek, Nucl. Instrum. Meth. A **420** (1999) 288.
- [33] Charu C. Aggarwal , Alexander Hinneburg , Daniel A. Keim, Proceedings of the 8th International Conference on Database Theory, p.420-434, January 04-06, 2001
- [34] <http://www.ai-junkie.com/ann/som/som1.html> and <http://davis.wpi.edu/~matt/courses/soms/>
- [35] C. Adloff *et al.* [H1 Collaboration], Eur. Phys. J. C **21** (2001) 33 [arXiv:hep-ex/0012053].
- [36] A. C. Benvenuti *et al.* [BCDMS Collaboration], Phys. Lett. B **223** (1989) 485.
- [37] A. C. Benvenuti *et al.* [BCDMS Collaboration], Phys. Lett. B **237** (1990) 592.
- [38] S. Chekanov *et al.* [ZEUS Collaboration], Eur. Phys. J. C **21** (2001) 443 [arXiv:hep-ex/0105090].

- [39] J. Pumplin, D. R. Stump, J. Huston, H. L. Lai, P. Nadolsky and W. K. Tung, JHEP **0207** (2002) 012 [arXiv:hep-ph/0201195].
- [40] <http://www.nikhef.nl/~h24/qcdnum/>
- [41] H. L. Lai *et al.* [CTEQ Collaboration], Eur. Phys. J. C **12** (2000) 375 [arXiv:hep-ph/9903282].
- [42] A. D. Martin, R. G. Roberts, W. J. Stirling and R. S. Thorne, Phys. Lett. B **531** (2002) 216 [arXiv:hep-ph/0201127].
- [43] M. Gluck, E. Reya and A. Vogt, Eur. Phys. J. C **5** (1998) 461 [arXiv:hep-ph/9806404].
- [44] H. L. Lai *et al.*, Phys. Rev. D **55**, 1280 (1997) [arXiv:hep-ph/9606399].